NANO LETTERS

pubs.acs.org/NanoLett Letter

Femtosecond Dynamics of a Polariton Bosonic Cascade at Room Temperature

Fei Chen,[¶] Hang Zhou,[¶] Hui Li,* Junhui Cao, Song Luo, Zheng Sun, Zhe Zhang, Ziqiu Shao, Fenghao Sun, Beier Zhou, Hongxing Dong, Huailiang Xu, Hongxing Xu, Alexey Kavokin, Zhanghai Chen,* and Jian Wu*

Cite This: *Nano Lett.* 2022, 22, 2023−2029 Read Online

ACCESS | Metrics & More | Article Recommendations | Supporting Information

ABSTRACT: Whispering gallery modes in a microwire are characterized by a nearly equidistant energy spectrum. In the strong exciton−photon coupling regime, this system represents a bosonic cascade: a ladder of discrete energy levels that sustains stimulated transitions between neighboring steps. Here, by using a femtosecond angle-resolved spectroscopic imaging technique, the ultrafast dynamics of polaritons in a bosonic cascade based on a one-dimensional ZnO whispering gallery microcavity are explicitly visualized. Clear ladder-form build-up processes from higher to lower energy branches of the polariton condensates are observed, which are well reproduced by modeling using rate equations. Remarkably, a pronounced superbunching feature, which could serve as solid evidence for bosonic cascades, is demonstrated by the measured second-order time correlation factor. In addition, the nonlinear polariton parametric scattering dynamics on a time scale of hundreds of femtoseconds are revealed. Our understandings pave the way toward ultrafast coherent control of polaritons at room temperature.

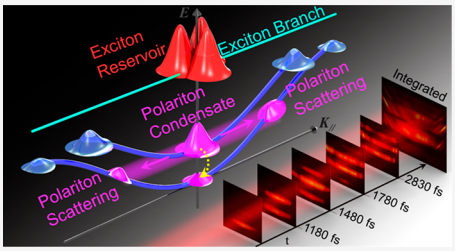

KEYWORDS: *exciton polariton, bosonic cascade, ultrafast dynamics, angle-resolved photoluminescence spectroscopy, second-order time correlation factor*

The strong coupling between excitons and cavity confined photons can lead to formation of hybrid half-light half-matter bosonic quasiparticles, i.e., the exciton−polaritons (EPs).[1,2] EPs bridge the gap between atomic physics and condensed matter physics by sharing many common characteristics with coupled atomic states. Phenomena such as Rabi splitting[3] and Bose−Einstein Condensation (BEC) in atomic systems can be found in the solid-state counterparts in a nonequilibrium regime.[4−6] When the interparticle distances decrease to the level of their de Broglie wavelengths, polaritons can accumulate massively on a single quantum state at high temperatures due to their extremely light effective masses.[7] Polariton condensates are of a unique driven-dissipative nature compared to conventional atomic BEC. They attract significant interests because of the recently discovered macroscopic coherent phenomena, including superfluidity,[8] vortex formation,[9−11] and soliton propagations.[12,13] Importantly, the excitonic constituent introduces strong coupling between polaritons through Coulomb interactions. This gives rise to a high nonlinearity in the interactions among polariton ensembles. Processes such as parametric scattering and bosonic amplification belong to this category.[14−17] In addition to the profound fundamental physics involved in polariton BEC, the condensates show excellent performances as low-cost light source elements,[18−23] ultrafast transistors and switches,[24−26] which are all central building blocks of polaritonic integrated devices.

Optically confined semiconductor structures such as microcavities, micropillars, microwires, etc., have an excellent potential for photonic band engineering. In the strong coupling regime, they can efficiently control the density of states of bosonic quasiparticles. Theoretical proposals based on specific designs of microsystems sustaining polariton modes include Berry phase interferometers,[27] polariton neurons,[28] polariton qubits,[29] bosonic cascades,[30] etc. Here we focus on the experimental realization of bosonic cascades, where stimulated transitions in a ladder of equidistant energy levels are expected to result in the generation of coherent radiation[31] and nonclassical light.[32] The relaxation processes in a bosonic cascade can be enhanced by bosonic stimulation thus giving rise to an extremely high quantum efficiency without the need to realize population inversion. They intrinsically differ from the Fermionic lasers. Attempts to the experimental realization of these effects with use of parabolic quantum wells embedded in planar microcavities[33] were not crowned by a decisive success so far.

Received: December 13, 2021
Revised: February 18, 2022
Published: February 24, 2022

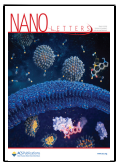

https://doi.org/10.1021/acs.nanolett.1c04800
Nano Lett. 2022, 22, 2023−2029

In this letter, we visualize the femtosecond dynamics of stimulated transitions of exciton−polaritons between the condensates formed by whispering gallery modes (WGM) of a ZnO microwire in the strong exciton-photon coupling regime. We demonstrate a room temperature bosonic cascade based on a one-dimensional (1D) ZnO microcavity. In our experiments, polariton condensates subsequently occupy four neighboring quantum states in a quasi-equidistant energy spectrum. The real time evolution of polariton condensates is characterized by multiple degrees of freedom involving energy and momentum. The processes of formation, relaxation as well as degenerate parametric scatterings of polariton condensates in a bosonic cascade are reported with an unprecedented time resolution. The ultrafast dynamics[34−41] can truly reveal the physics of bosonic cascades that has not been fully understood until now. Our findings make a step forward in understanding of dynamics of many-body bosonic systems and offer the possibility to realize coherent manipulations, which may also promote the application of integrated polaritonic devices operating at room temperature.

The photoluminescence (PL) measurements for the steady states typically show a very complex pattern (presented in Figure 1a and 2a) in which the superposed processes are hard

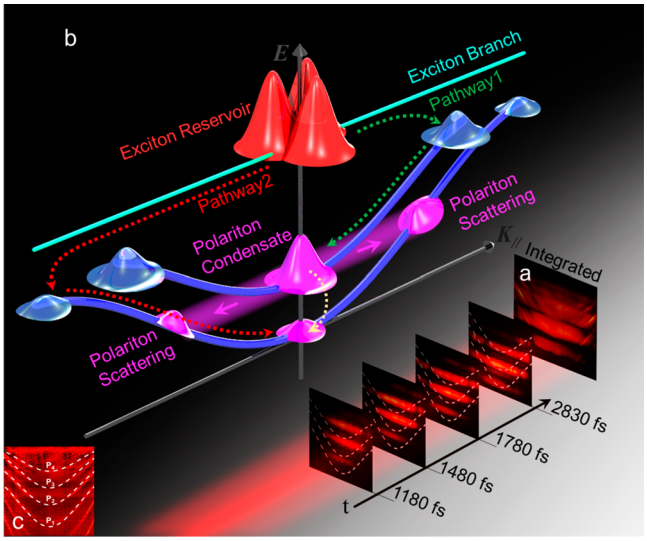

Figure 1. Schematic illustration of polariton dynamics in a Bosonic cascade. (a) Femtosecond angle-resolved spectroscopic imaging (FARSI) measurement. (b) Schematic drawing of the polariton condensation and parametric scattering dynamics. (c) Dispersion mapping of the ZnO WGM obtained at an excitation power below the condensation threshold. Dashed curves are the fitting results for the LP branches labeled as P_{1-4}, respectively.

to be disentangled. By using the femtosecond angle-resolved spectroscopic imaging (FARSI) technique, the dynamics of polariton condensation on multiple lower polariton (LP) branches, as well as the complex parametric scattering processes, can be clearly visualized. The underlying dynamics of polariton condensation formed in 1D ZnO WGM are schematically shown in Figure 1b. At the leading edge of the femtosecond excitation pulse, exciton reservoir can be ignited almost instantly at femtosecond time scales. The density of the exciton reservoir grows as the field strength of the pumping pulse increases. The repulsive interactions between excitons become efficient and the excitons can be scattered to the surroundings. As the exciton reservoir relaxes, the screening effect on the cavity polaritonic system changes gradually and thus will result in a time-dependent shift of the detuning between exciton and cavity photon modes, which eventually affects the polariton condensation dynamics.[42] Early study based on the ZnO microwire pointed out that the competition between media loss and cavity loss would give rise to an optimized WGM with the highest quality factor (Q-factor).[43] Polariton condensates are preferentially formed on such optimized mode. The exciton reservoir holding a large population can be strongly coupled to a cavity mode exhibiting high Q-factor to form polaritons on a certain LP branch, i.e., along Pathway 1 presented in Figure 1b. As the exciton reservoir relaxes, polaritons on the next LP branch with lower energy can be built from the exciton reservoir through Pathway 2. These polaritons experience evaporate cooling through polariton−phonon and polariton−polariton interactions and will gradually decay down to the ground state.[44] When a threshold density is exceeded, a huge number of polaritons will massively accumulate onto one single quantum state, thus forming a condensate.

It is theoretically predicted that the bosonic ensemble on these nearly equidistant LP branches can transit through the energy ladders, where the quantum statistics of bosonic cascade exhibits superbunching feature[32] evidenced by a second-order correlation factor larger than 2. Such bosonic cascading processes could dramatically influence the whole dynamics of the polariton condensation in a 1D ZnO microcavity. A ladder-form polariton condensation from higher to lower energy LP branches is expected that constitutes an evidence for the bosonic cascade effect.

The steady-state dispersion mapping of the ZnO microwire is presented in Figure 1c with multiple LP branches (marked by P_{1-4}) obtained from the plane wave model.[45] Polariton condensation formation and relaxation on the four distinct LP branches are recorded with a time resolution of about 30 fs for an excitation strength of $5P_{th}$ (P_{th} is the threshold power for condensation formation). The time-integrated PL distribution as a function of energy and momentum (shown in Figure 2a) exhibits a complex pattern. This corresponds to the superposition of the dynamical PL emission from the multiple LP branches. The strong emission in the middle around $k_{\parallel} = 0$ is from the polariton condensates on various LP modes, where the broadening of the signal in the k-space (as can be seen in Figure 1a) can be attributed to the transient polariton−polariton interactions. In the time-resolved measurement, a ladder-form buildup of the PL distributions from polariton condensation starting from the highest LP branch P_4 and successively transiting toward the lower energy branches, i.e., P_{3-1}, are shown explicitly in Figure 2b. The time delays between the adjacent branches are found to be around hundreds of femtoseconds (τ_{43}: −100 fs; τ_{32}: 310 fs; τ_{21}: 110 fs. Here the τ_{ij} represents the time interval between the maximum population for the ith and the jth LP branch). The resulting polariton dynamics undergo redshifts with different characteristic times.

The calculation results are compared with the experimental data and are shown in Figure 2c, where a good agreement has been achieved. In our simulation, the detuning-dependent effect is considered by fitting the Q-factor for different energies at various LP branches. From that we can obtain empirical decay rates γ_k for the four LP branches.[43] Optimization of all the other fitting parameters is achieved by using the genetic

https://doi.org/10.1021/acs.nanolett.1c04800
Nano Lett. 2022, 22, 2023−2029

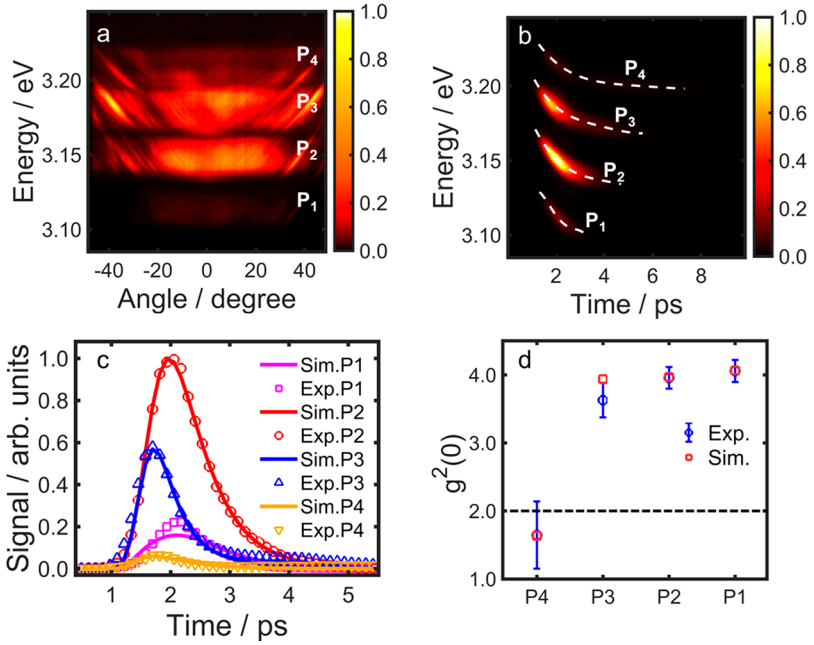

Figure 2. Polariton condensation dynamics and the second-order time correlation measurement. (a) Time-integrated 2D imaging of the PL distributions with the pump power at $P = 5P_{th}$. (b) Time-dependent PL distribution in the energy degree of freedom for the four branches. The dashed curve helps to guide the eyes. (c) Simulated and experimental results for time-dependent populations of the polariton condensates for the four LP branches. (d) Derived second-order time correlation factor, $g^{(2)}(0)$, for the LP branches P_{1-4} obtained from experiment and theoretical calculations. The dashed line lying at $g^{(2)}(0) = 2$ indicates the division for classical light and superbunching effects.

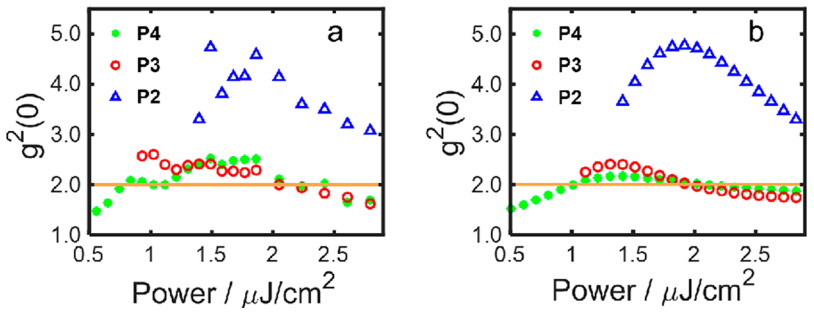

Figure 3. (a) Measured and (b) calculated pump power-dependence of the $g^{(2)}(0)$ factor obtained in a ZnO microcavity at room temperature.

algorithm. The observed very first buildup of polariton condensate on the P_3 branch can be originated from the fact that the P_3 branch lies around the optimized wavelength range with the maximum Q-factor. The succeeding signals on P_2 and P_1 are in agreement with the theoretical model accounting for the cascading effect. A slight deviation for the P_1 branch approaching the end of the multibranch build-up process might be from the oversimplified approximation in our theoretical model or from the imperfection of the ZnO microwire. In our measurements, each polariton condensate formed on the P_{1-4} branches lasts for 560−860 fs. It indicates that each branch outputs a polariton lasing signal with a femtosecond pulse duration.

The mechanism of bosonic cascade is demonstrated by the extracted second-order time correlation factor $g^{(2)}(0)$ for all the LP branches.[46] The $g^{(2)}$ functions are widely used to provide direct insight into the quantum fluctuations of polariton condensates.[6,46,47] In many cases, the extraction of $g^{(2)}(\tau)$ requires autocorrelation measurements where a Hanbury Brown and Twiss (HBT) setup[48] is utilized. The second-order time correlation function is defined as

$$g^{(2)}(\tau) = \langle I(t+\tau)I(t)\rangle/[\langle I(t+\tau)\rangle\langle I(t)\rangle] \quad (1)$$

where $I(t)$ is the polariton emission intensity at time t, and $\langle\cdots\rangle$ indicates the time averaging. A classical Bose gas at the thermal equilibrium that satisfies a Boltzmann distribution is characterized by $g^{(2)}(0) = 2$. According to ref 32, a $g^{(2)}$ factor larger than 2 representing a superbunching property is the intrinsic feature of the quantum statistics for the bosonic cascades. In our experiment, polariton emission as a function of time is explicitly detected using the FARSI technique. The measured signal on each LP branch is extracted and integrated over the energy degree of freedom. The resulting signal is then projected to the time axis to produce $I(t)$ for the P_{1-4} branches. $g^{(2)}(0)$ values are calculated according to eq 1. We have obtained $g^{(2)}(0) > 2$ for the P_{3-1} branches in the measurement, i.e., 1.6 (P_4), 3.6 (P_3), 3.9 (P_2), and 4.0 (P_1), as explicitly presented in Figure 2d. Theoretically, the quantum Boltzmann master equations[32] used to calculate the $g^{(2)}(0)$ demonstrate an excellent agreement with these experimental results (for the theoretical details, please see Section IV in the Supporting Information[49]). The $g^{(2)}(0) < 2$ for the P_4 branch might be attributed to the fast transition of this highest energy

https://doi.org/10.1021/acs.nanolett.1c04800
Nano Lett. 2022, 22, 2023−2029

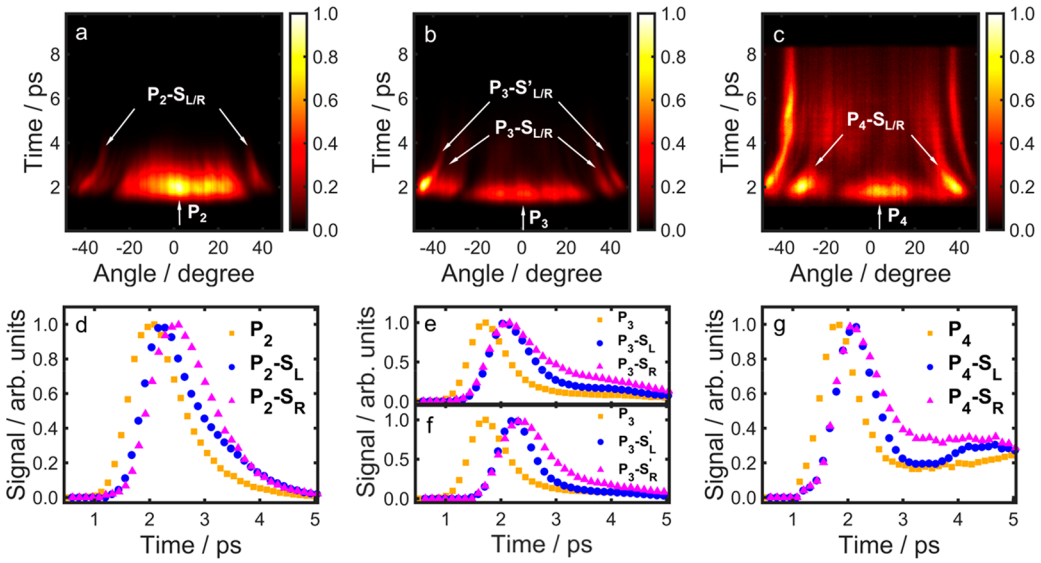

Figure 4. Polariton parametric scattering dynamics. (a–c) PL as a function of emission angle and time extracted for the $P_{2,3,4}$ branches in the momentum space, respectively (at $P = 5P_{th}$). (d–g) Corresponding time-resolved signal by projecting the data onto the time axis for the selected regions indicated in parts a–c. The dynamics of the scattering source close to the center (labeled as P_{2-4}) and the scattered parts (labeled as P_{2-4}-$S_{L/R}$) are plotted separately, showing characteristic delays.

branch toward lower energy branches. The initial occupation of P_4 forms a mixed state of both coherent and thermal statistics, resulting in a $g^{(2)}(0)$ factor in the region between 1 and 2. Superbunching is hard to be achieved in this branch due to the fast optical decay and transition of polaritons to the P_3 branch. In contrast, all the other branches can be fed efficiently by the stimulated cascaded transitions.

The pump power-dependence of $g^{(2)}(0)$ has been measured, and the results are in good agreement with the theoretical modeling based on the quantum Boltzmann master equations written for a four-level bosonic cascade[32] (as shown in Figure 3). At low pumping power, only few excitons exist in this system, and the transition rate between different energy levels is very low, so that the statistics of polaritons is governed by the pumping rather than by relaxation. In contrast, while the power increases, the second-order correlation starts to grow above 2 and it reaches its maximum at the pump power of around 1.9 μJ cm^{-2}. With a further increase of the pump power, the number of excitons in the reservoir becomes quite large so that the reservoir starts replenishing the cascades continuously. Hence the coherence induced by the transitions between different energy levels in the cascade starts playing a less important role. As a result, $g^2(0)$ tends to reduce to the value of 2 representing characteristic of a thermal distribution of polaritons. The $g^{(2)}(0)$ factors are above 2 in a certain pump power range, confirming the dominance of cascading process.

Polariton parametric scatterings (PPS) can induce entangled signal and idler ensembles, which is why it is highly important for applications in quantum information processing.[17,50,51] The polariton condensates in 1D microcavity are ideal sources for parametric scattering, due to the existence of rich interbranch scattering channels and easy implementation of the phase matching condition. Complex scattering processes in 1D ZnO WGM have been predicted theoretically.[52] However, due to the harsh requirement for time resolution, the subpicosecond scattering dynamics have not been resolved experimentally. Here we boost up the time resolution down to femtoseconds and explicitly show the ultrafast dynamics of the PPS processes in 1D ZnO WGM at room temperature.

In Figure 4, the time-resolved momentum distributions of the polariton condensates are illustrated for the P_{2-4} branches, respectively. The scattered signal and idler pairs (labeled with $S_{L/R}$) at both sides of the condensate with degenerate energy and opposite momentum can be recognized. After an ultrafast injection, the formation of polariton condensation close to the ground state takes hundreds of femtoseconds to arrive at the maximum population. During this time, the momentum distributions of the condensate become broadened as the polariton–polariton interactions are enhanced (as shown in Figure 4a–c). After reaching the peak population, the momentum distribution of the polaritons in each LP branch experiences a clear shrinking. Both the build-up and the relaxation are accompanied by a time-dependent redshift observed in the energy domain (shown in Figure 2b). In general, polariton condensates are formed first at the ground states of a given LP branch, and part of the polaritons can be scattered parametrically toward the adjacent LP branches after hundreds of femtoseconds, as schematically illustrated in Figure 1b. The lagging time can be clearly illustrated by projecting the signals in Figures 4a–c onto the time axis. As shown in Figure 4d, the magenta and the blue data represent the scattered signals to emission angles around ±36.3° from the P_2 branch. The peak positions of the scattered signals are delayed with respect to the source emitted at around 0° (presented by the yellow squares) by about 360 fs. Comparable features of the scattering pairs can be recognized for another LP branch P_4 as shown in Figure 4g, where the scattering happens in around 290 fs. Particularly, the parametric scattering toward the next two neighboring branches is observed for the huge polariton condensates initially formed on the P_3 branch. A longer delay of about 590 fs can be found for the scattering pairs observed at around ±42.7° (shown in Figure 4f), compared to the 390 fs delay time obtained for the scattering pairs at around ±34.7° (shown in Figure 4e).

https://doi.org/10.1021/acs.nanolett.1c04800
Nano Lett. 2022, 22, 2023–2029

In summary, we have visualized the femtosecond dynamics of polariton condensation in a bosonic cascade at room temperature in a 1D ZnO WGM using the FARSI technique. The cascading build-up process of the polariton condensation from higher to lower energy LP branches is documented for various excitation powers. The characteristic build-up and relaxation times of polariton condensation on each of the steps of the cascade are obtained with femtosecond resolutions which can be precisely tailored by the optical excitation conditions. Theoretical simulations have shown that the bosonic cascading effect plays an inevitable role in the whole dynamics. The second-order time correlation factor $g^{(2)}(0)$ experimentally measured for the various LP branches demonstrates a pronounced superbunching effect. In addition, the ultrafast dynamics of rich parametric scattering channels are distinguished, where the scattered signals toward the adjacent LP branches are blooming with a lagging time of hundreds of femtoseconds with respect to their scattering sources. These dynamics are original and go beyond the theoretical expectations for the bosonic cascade dynamics that did not consider subbands associated with every step of the ladder.[30−33] The highly efficient parametric scattering channels discovered here can be applied potentially in quantum information processing. Our work unveils the details of femtosecond dynamics of polariton condensation in an extreme time domain.

METHODS

Experimental Setup. Femtosecond laser pulses at the central wavelength of 350 nm are used to nonresonantly excite the ZnO microwire, and the femtosecond angle-resolved spectroscopic imaging (FARSI) technique is developed to explore the ultrafast dynamics of polariton condensation.[53] The photoluminescence (PL) in both the energy and momentum degrees of freedom can be visualized frame by frame with femtosecond time resolutions via the TE polarization which dominates the whole spectra. The possible dispersions raised by related optical elements have been carefully corrected. See the Supporting Information[49] for more details of the experimental technique.

Theoretical Model. The here-observed underlying dynamics are confirmed by the modeling using rate equations[30,49,54,55] involving the bosonic cascading effect. The equations can be written as

$$P(t) = P_0 \exp[-(t - t_{offset})^2/2\sigma^2] \tag{2}$$

$$\frac{\partial n_R}{\partial t} = P(t) - \gamma_R n_R - \sum_{i=1}^{4} R_i n_R (n_i + 1) \tag{3}$$

$$\frac{\partial n_4}{\partial t} = -\gamma_4 n_4 + R_4 n_R (n_4 + 1) - R_{43} n_4 (n_3 + 1) \tag{4}$$

$$\frac{\partial n_k}{\partial t} = -\gamma_k n_k + R_k n_R (n_k + 1) + R_{(k+1)k} n_{k+1} (n_k + 1) - R_{k(k-1)} n_k (n_{k-1} + 1) \tag{5}$$

$$\frac{\partial n_1}{\partial t} = -\gamma_1 n_1 + R_1 n_R (n_1 + 1) + R_{21} n_2 (n_1 + 1) \tag{6}$$

$$\frac{\partial n_{THz}}{\partial t} = -\gamma_{THz} n_{THz} + \sum_{k=2}^{4} R_{k(k-1)} n_k (n_{k-1} + 1) \tag{7}$$

$$R_{k(k-1)} = r_{k(k-1)} (n_{THz} + 1) \tag{8}$$

where $P(t)$ is the pump power. n_R and γ_R represent the density and the decay rate of the exciton reservoir, respectively. n_k (k = 1−4) represents the polariton density on the LP branches of P_k, and γ_k is the corresponding decay rate. The decay rates for the different LP branches, γ_{1-4}, are extracted according to ref 43, with γ_4 = 2.238 ps^{-1}, γ_3 = 1.852 ps^{-1}, γ_4 = 1.925 ps^{-1}, and γ_1 = 2.112 ps^{-1}. R_k (k = 1−4) stands for the scattering rate from the exciton reservoir to the kth LP branch P_k. The parameters obtained in the calculation are R_4 = 0.064 ps^{-1}, R_3 = 0.328 ps^{-1}, R_2 = 0.294 ps^{-1}, and R_1 = 0.089 ps^{-1}, respectively. R_{ij} represents the interbranch scattering rate between the adjacent LP branches, i.e., indicating the bosonic cascading effect. They are R_{43} = 0.047 ps^{-1}, R_{32} = 0.364 ps^{-1}, and R_{21} = 0.148 ps^{-1}, respectively. n_{THz} is the THz mode occupation, and γ_{THz} (around 100 ps^{-1}) is the corresponding decay rate.

ASSOCIATED CONTENT

Supporting Information

The Supporting Information is available free of charge at https://pubs.acs.org/doi/10.1021/acs.nanolett.1c04800.

Additional information on material, experimental setup, theoretical calculations for multimode coupling, and the power-dependence of the second-order time correlation function (PDF)

AUTHOR INFORMATION

Corresponding Authors

Hui Li − *State Key Laboratory of Precision Spectroscopy, East China Normal University, Shanghai 200062, China;* orcid.org/0000-0003-0927-8124; Email: hli@lps.ecnu.edu.cn

Zhanghai Chen − *Department of Physics, College of Physical Science and Technology, Xiamen University, Xiamen 361005, China*; Email: zhanghai@xmu.edu.cn

Jian Wu − *State Key Laboratory of Precision Spectroscopy, East China Normal University, Shanghai 200062, China; Collaborative Innovation Center of Extreme Optics, Shanxi University, Taiyuan, Shanxi 030006, China; CAS Center for Excellence in Ultra-intense Laser Science, Shanghai 201800, China*; Email: jwu@phy.ecnu.edu.cn

Authors

Fei Chen − *State Key Laboratory of Precision Spectroscopy, East China Normal University, Shanghai 200062, China*

Hang Zhou − *Department of Physics, College of Physical Science and Technology, Xiamen University, Xiamen 361005, China*

Junhui Cao − *School of Science, Westlake University, Zhejiang 310024, China; Institute of Natural Sciences, Westlake Institute for Advanced Study, Zhejiang 310024, China*

Song Luo − *Department of Physics, College of Physical Science and Technology, Xiamen University, Xiamen 361005, China*

Zheng Sun − *State Key Laboratory of Precision Spectroscopy, East China Normal University, Shanghai 200062, China;* orcid.org/0000-0002-5209-2563

https://doi.org/10.1021/acs.nanolett.1c04800
Nano Lett. 2022, 22, 2023−2029

Zhe Zhang − *State Key Laboratory of Precision Spectroscopy, East China Normal University, Shanghai 200062, China; Department of Physics, College of Physical Science and Technology, Xiamen University, Xiamen 361005, China; Collaborative Innovation Center of Extreme Optics, Shanxi University, Taiyuan, Shanxi 030006, China; CAS Center for Excellence in Ultra-intense Laser Science, Shanghai 201800, China; School of Science, Westlake University, Zhejiang 310024, China; Institute of Natural Sciences, Westlake Institute for Advanced Study, Zhejiang 310024, China; Shanghai Institute of Optics and Fine Mechanics, Chinese Academy of Sciences, Shanghai 201800, China*

Ziqiu Shao − *School of Science, Westlake University, Zhejiang 310024, China; Institute of Natural Sciences, Westlake Institute for Advanced Study, Zhejiang 310024, China*

Fenghao Sun − *State Key Laboratory of Precision Spectroscopy, East China Normal University, Shanghai 200062, China;* orcid.org/0000-0003-0210-5204

Beier Zhou − *Shanghai Institute of Optics and Fine Mechanics, Chinese Academy of Sciences, Shanghai 201800, China*

Hongxing Dong − *Shanghai Institute of Optics and Fine Mechanics, Chinese Academy of Sciences, Shanghai 201800, China*

Huailiang Xu − *State Key Laboratory of Precision Spectroscopy, East China Normal University, Shanghai 200062, China*

Hongxing Xu − *State Key Laboratory of Precision Spectroscopy, East China Normal University, Shanghai 200062, China;* orcid.org/0000-0002-1718-8834

Alexey Kavokin − *School of Science, Westlake University, Zhejiang 310024, China; Institute of Natural Sciences, Westlake Institute for Advanced Study, Zhejiang 310024, China;* orcid.org/0000-0003-2713-1062

Complete contact information is available at: https://pubs.acs.org/10.1021/acs.nanolett.1c04800

Author Contributions

[¶]F.C. and H.Z. contributed equally. J.W., Z.C., and H.L. conceived the idea and initiated the study. F.C., H.L., S.L., Z.Z., and F.S. conducted the experimental work. H.Z., A.K., F.C., J.C., and Z.Q.S. performed the simulations. All authors contributed to the data analysis and writing the manuscript. J.W., Z.C., and H.L. supervised and guided the work.

Notes

The authors declare no competing financial interest.

ACKNOWLEDGMENTS

We thank Dr. Z. Wang for the fruitful discussions. This work is supported by the National Key R&D Program of China (Grant Nos. 2018YFA0306303 and 2018YFA0306304), the National Natural Science Fund (Grant Nos. 92050105, 91950201, 11834004, 11674069, and 11574205), the project supported by the Shanghai Committee of Science and Technology, China (Grant Nos. 22ZR1419700, 19ZR1473900, and 19JC1412200), and the Shanghai Municipal Science and Technology Major Project. A.K. acknowledges Project No. 041020100118 supported by Westlake University and Programme 2018R01002 funded by the Leading Innovative and Entrepreneur Team Introduction Programme of Zhejiang.

REFERENCES

(1) Kavokin, A. V.; Malpuech, G. *Cavity Polaritons*; Elsevier, Amsterdam, 2003.

(2) Hopfield, J. J. Theory of the Contribution of Excitons to the Complex Dielectric Constant of Crystals. *Phys. Rev.* **1958**, *112* (5), 1555.

(3) Weisbuch, C.; Nishioka, M.; Ishikawa, A.; Arakawa, Y. Observation of the coupled exciton-photon mode splitting in a semiconductor quantum microcavity. *Phys. Rev. Lett.* **1992**, *69* (23), 3314.

(4) Kasprzak, J.; Richard, M.; Kundermann, S.; Baas, A.; Jeambrun, P.; Keeling, J. M. J.; Marchetti, F. M.; Szymanska, M. H.; Andre, R.; Staehli, J. L.; Savona, V.; et al. Bose−Einstein condensation of exciton polaritons. *Nature* **2006**, *443* (7110), 409−414.

(5) Balili, R.; Hartwell, V.; Snoke, D.; Pfeiffer, L.; West, K. Bose−Einstein condensation of microcavity polaritons in a trap. *Science* **2007**, *316* (5827), 1007−1010.

(6) Deng, H.; Weihs, G.; Santori, C.; Bloch, J.; Yamamoto, Y. Condensation of semiconductor microcavity exciton polaritons. *Science* **2002**, *298* (5591), 199−202.

(7) Byrnes, T.; Kim, N. Y.; Yamamoto, Y. Exciton-polariton condensates. *Nat. Phys.* **2014**, *10* (11), 803−813.

(8) Amo, A.; Sanvitto, D.; Laussy, F. P.; Ballarini, D.; del Valle, E.; Martin, M. D.; Lemaitre, A.; Bloch, J.; Krizhanovskii, D. N.; Skolnick, M. S.; Tejedor, C.; et al. Collective fluid dynamics of a polariton condensate in a semiconductor microcavity. *Nature* **2009**, *457* (7227), 291−295.

(9) Lagoudakis, K. G.; Wouters, M.; Richard, M.; Baas, A.; Carusotto, I.; Andre, R.; Dang, L.; Deveaud-Pledran, B. Quantized vortices in an exciton-polariton condensate. *Nat. Phys.* **2008**, *4* (9), 706−710.

(10) Lagoudakis, K. G.; Ostatnicky, T.; Kavokin, A. V.; Rubo, Y. G.; Andre, R.; Deveaud-Pledran, B. Observation of half-quantum vortices in an exciton-polariton condensate. *Science* **2009**, *326* (5955), 974−976.

(11) Nardin, G.; Grosso, G.; Leger, Y.; Pietka, B.; Morier-Genoud, F.; Deveaud-Pledran, B. Hydrodynamic nucleation of quantized vortex pairs in a polariton quantum fluid. *Nat. Phys.* **2011**, *7* (8), 635−641.

(12) Amo, A.; Pigeon, S.; Sanvitto, D.; Sala, V. G.; Hivet, R.; Carusotto, I.; Pisanello, F.; Lemenager, G.; Houdre, R.; Giacobino, E.; Ciuti, C.; et al. Polariton superfluids reveal quantum hydrodynamic solitons. *Science* **2011**, *332* (6034), 1167−1170.

(13) Sich, M.; Krizhanovskii, D. N.; Skolnick, M. S.; Gorbach, A. V.; Hartley, R.; Skryabin, D. V.; Cerda-Mendez, E. A.; Biermann, K.; Hey, R.; Santos, P. V. Observation of bright polariton solitons in a semiconductor microcavity. *Nat. Photonics* **2012**, *6* (1), 50−55.

(14) Kuwata-Gonokami, M.; Inouye, S.; Suzuura, H.; Shirane, M.; Shimano, R.; Someya, T.; Sakaki, H. Parametric scattering of cavity polaritons. *Phys. Rev. Lett.* **1997**, *79* (7), 1341−1344.

(15) Messin, G.; Karr, J. P.; Baas, A.; Khitrova, G.; Houdre, R.; Stanley, R. P.; Oesterle, U.; Giacobino, E. Parametric polariton amplification in semiconductor microcavities. *Phys. Rev. Lett.* **2001**, *87* (12), 127403.

(16) Savvidis, P. G.; Ciuti, C.; Baumberg, J. J.; Whittaker, D. M.; Skolnick, M. S.; Roberts, J. S. Off-branch polaritons and multiple scattering in semiconductor microcavities. *Phys. Rev. B* **2001**, *64* (7), No. 075311.

(17) Xie, W.; Dong, H. X.; Zhang, S. F.; Sun, L. X.; Zhou, W. H.; Ling, Y. J.; Lu, J.; Shen, X. C.; Chen, Z. H. Room-temperature polariton parametric scattering driven by a one-dimensional polariton condensate. *Phys. Rev. Lett.* **2012**, *108* (16), 166401.

(18) Deng, H.; Weihs, G.; Snoke, D.; Bloch, J.; Yamamoto, Y. Polariton lasing vs. photon lasing in a semiconductor microcavity. *Proc. Natl. Acad. Sci. U. S. A.* **2003**, *100* (26), 15318−15323.

(19) Tsintzos, S. I.; Pelekanos, N. T.; Konstantinidis, G.; Hatzopoulos, Z.; Savvidis, P. G. A GaAs polariton light-emitting diode operating near room temperature. *Nature* **2008**, *453* (7193), 372−375.

(20) Bhattacharya, P.; Xiao, B.; Das, A.; Bhowmick, S.; Heo, J. Solid state electrically injected exciton-polariton laser. *Phys. Rev. Lett.* **2013**, *110* (20), 206403.
(21) Tsintzos, S. I.; Savvidis, P. G.; Deligeorgis, G.; Hatzopoulos, Z.; Pelekanos, N. T. Room temperature GaAs exciton-polariton light emitting diode. *Appl. Phys. Lett.* **2009**, *94* (7), No. 071109.
(22) Su, R.; Diederichs, C.; Wang, J.; Liew, T. C. H.; Zhao, J. X.; Liu, S.; Xu, W. G.; Chen, Z. H.; Xiong, Q. H. Room-temperature polariton lasing in all-inorganic perovskite nanoplatelets. *Nano Lett.* **2017**, *17* (6), 3982−3988.
(23) Zhang, Z.; Wang, Y.; Yin, S.; Hu, T.; Wang, Y.; Liao, L.; Luo, S.; Wang, J.; Zhang, X.; Ni, P.; Shen, X.; et al. Exciton-polariton light-emitting diode based on a ZnO microwire. *Opt. Express* **2017**, *25* (15), 17375−17381.
(24) Ballarini, D.; De Giorgi, M.; Cancellieri, E.; Houdre, R.; Giacobino, E.; Cingolani, R.; Bramati, A.; Gigli, G.; Sanvitto, D.; et al. All-optical polariton transistor. *Nat. Commun.* **2013**, *4* (1), 1778.
(25) Zasedatelev, A. V.; Baranikov, A. V.; Urbonas, D.; Scafirimuto, F.; Scherf, U.; Stoferle, T.; Mahrt, R. F.; Lagoudakis, P. G. A room-temperature organic polariton transistor. *Nat. Photonics* **2019**, *13* (6), 378−383.
(26) Dreismann, A.; Ohadi, H.; del Valle-Inclan Redondo, Y.; Balili, R.; Rubo, Y. G.; Tsintzos, S. I.; Deligeorgis, G.; Hatzopoulos, Z.; Savvidis, P. G.; Baumberg, J. J. A sub-femtojoule electrical spin-switch based on optically trapped polariton condensates. *Nat. Mater.* **2016**, *15* (10), 1074−1078.
(27) Shelykh, I. A.; Pavlovic, G.; Solnyshkov, D. D.; Malpuech, G. Proposal for a Mesoscopic Optical Berry-Phase Interferometer. *Phys. Rev. Lett.* **2009**, *102* (4), No. 046407.
(28) Liew, T. C. H.; Kavokin, A. V.; Shelykh, I. A. Optical circuits based on polariton neurons in semiconductor microcavities. *Phys. Rev. Lett.* **2008**, *101* (1), No. 016402.
(29) Xue, Y.; Chestnov, I.; Sedov, E.; Kiktenko, E.; Fedorov, A. K.; Schumacher, S.; Ma, X.; Kavokin, A. Split-ring polariton condensates as macroscopic two-level quantum systems. *Phys. Rev. Research* **2021**, *3* (1), No. 013099.
(30) Liew, T. C. H.; Glazov, M. M.; Kavokin, K. V.; Shelykh, I. A.; Kaliteevski, M. A.; Kavokin, A. V. Proposal for a bosonic cascade laser. *Phys. Rev. Lett.* **2013**, *110* (4), No. 047402.
(31) Pervishko, A. A.; Liew, T. C. H.; Kavokin, A. V.; Shelykh, I. A. Bistability in bosonic terahertz lasers. *J. Phys: Condensed Matter* **2014**, *26* (8), No. 085303.
(32) Liew, T. C. H.; Rubo, Y. G.; Sheremet, A. S.; De Liberato, S.; Shelykh, I. A.; Laussy, F. P.; Kavokin, A. V. Quantum statistics of bosonic cascades. *New J. Phys.* **2016**, *18* (2), No. 023041.
(33) Trifonov, A. V.; Cherotchenko, E. D.; Carthy, J. L.; Ignatiev, I. V.; Tzimis, A.; Tsintzos, S.; Hatzopoulos, Z.; Savvidis, P. G.; Kavokin, A. V. Dynamics of the energy relaxation in a parabolic quantum well laser. *Phys. Rev. B* **2016**, *93* (12), 125304.
(34) Tosi, G.; Christmann, G.; Berloff, N. G.; Tsotsis, P.; Gao, T.; Hatzopoulos, Z.; Savvidis, P. G.; Baumberg, J. J. Sculpting oscillators with light within a nonlinear quantum fluid. *Nat. Phys.* **2012**, *8* (3), 190−194.
(35) Dominici, L.; Petrov, M.; Matuszewski, M.; Ballarini, D.; De Giorgi, M.; Colas, D.; Cancellieri, E.; Silva Fernandez, B. S.; Bramati, A.; Gigli, G.; Kavokin, A.; et al. Real-space collapse of a polariton condensate. *Nat. Commun.* **2015**, *6* (1), 8993.
(36) del Valle, E.; Sanvitto, D.; Amo, A.; Laussy, F. P.; Andre, R.; Tejedor, C.; Vina, L. Dynamics of the Formation and Decay of Coherence in a Polariton Condensate. *Phys. Rev. Lett.* **2009**, *103* (9), No. 096404.
(37) Wertz, E.; Amo, A.; Solnyshkov, D. D.; Ferrier, L.; Liew, T. C. H.; Sanvitto, D.; Senellart, P.; Sagnes, I.; Lemaitre, A.; Kavokin, A. V.; Malpuech, G.; et al. Propagation and Amplification Dynamics of 1D Polariton Condensates. *Phys. Rev. Lett.* **2012**, *109* (21), 216404.
(38) De Giorgi, M.; Ballarini, D.; Cazzato, P.; Deligeorgis, G.; Tsintzos, S. I.; Hatzopoulos, Z.; Savvidis, P. G.; Gigli, G.; Laussy, F. P.; Sanvitto, D. Relaxation Oscillations in the Formation of a Polariton Condensate. *Phys. Rev. Lett.* **2014**, *112* (11), 113602.
(39) Dominici, L.; Colas, D.; Donati, S.; Restrepo Cuartas, J. P.; De Giorgi, M.; Ballarini, D.; Guirales, G.; Lopez Carreno, J. C.; Bramati, A.; Gigli, G.; del Valle, E.; et al. Ultrafast Control and Rabi Oscillations of Polaritons. *Phys. Rev. Lett.* **2014**, *113* (22), 226401.
(40) Sich, M.; Chana, J. K.; Egorov, O. A.; Sigurdsson, H.; Shelykh, I. A.; Skryabin, D. V.; Walker, P. M.; Clarke, E.; Royall, B.; Skolnick, M. S.; Krizhanovskii, D. N. Transition from Propagating Polariton Solitons to a Standing Wave Condensate Induced by Interactions. *Phys. Rev. Lett.* **2018**, *120* (16), 167402.
(41) Anton, C.; Liew, T. C. H.; Tosi, G.; Martin, M. D.; Gao, T.; Hatzopoulos, Z.; Eldridge, P. S.; Savvidis, P. G.; Vina, L. Dynamics of a polariton condensate transistor switch. *Appl. Phys. Lett.* **2012**, *101* (26), 261116.
(42) Gay, J. G. Screening of excitons in semiconductors. *Phys. Rev. B* **1971**, *4* (8), 2567−2575.
(43) Hu, T.; Xie, W.; Wu, L.; Wang, Y. F.; Zhang, L.; Chen, Z. H. Optimized polaritonic modes in whispering gallery microcavities. *Solid State Commun.* **2017**, *262* (1), 7−10.
(44) Wang, J.; Xie, W.; Zhang, L.; Xu, D.; Liu, W.; Lu, J.; Wang, Y.; Gu, J.; Chen, Y.; Shen, X.; Chen, Z. Exciton-polariton condensate induced by evaporative cooling in a three-dimensionally confined microcavity. *Phys. Rev. B* **2015**, *91* (16), 165423.
(45) Nobis, T.; Kaidashev, E. M.; Rahm, A.; Lorenz, M.; Grundmann, M. Whispering gallery modes in nanosized dielectric resonators with hexagonal cross section. *Phys. Rev. Lett.* **2004**, *93* (10), 103903.
(46) Kasprzak, J.; Richard, M.; Baas, A.; Deveaud, B.; Andre, R.; Poizat, J. P.; Dang, L. S. Second-Order Time Correlations within a Polariton Bose−Einstein Condensate in a CdTe Microcavity. *Phys. Rev. Lett.* **2008**, *100* (6), No. 067402.
(47) Love, A. P. D.; Krizhanovskii, D. N.; Whittaker, D. M.; Bouchekioua, R.; Sanvitto, D.; Al Rizeiqi, S.; Bradley, R.; Skolnick, M. S.; Eastham, P. R.; Andre, R.; Dang, L. S. Intrinsic Decoherence Mechanisms in the Microcavity Polariton Condensate. *Phys. Rev. Lett.* **2008**, *101* (6), No. 067404.
(48) Brown, R. H.; Twiss, R. Correlation between Photons in two Coherent Beams of Light. *Nature (London)* **1956**, *177* (4497), 27−29.
(49) See the Supporting Information for details of the experimental and simulation methods.
(50) Kundermann, S.; Saba, M.; Ciuti, C.; Guillet, T.; Oesterle, U.; Staehli, J. L.; Deveaud, B. Coherent control of polariton parametric scattering in semiconductor microcavities. *Phys. Rev. Lett.* **2003**, *91* (10), 107402.
(51) Romanelli, M.; Leyder, C.; Karr, J. P.; Giacobino, E.; Bramati, A. Four wave mixing oscillation in a semiconductor microcavity: Generation of two correlated polariton populations. *Phys. Rev. Lett.* **2007**, *98* (10), 106401.
(52) Dietrich, C. P.; Johne, R.; Michalsky, T.; Sturm, C.; Eastham, P.; Franke, H.; Lange, M.; Grundmann, M.; Schmidt-Grund, R. Parametric relaxation in whispering gallery mode exciton-polariton condensates. *Phys. Rev. B* **2015**, *91* (4), No. 041202.
(53) Chen, F.; Li, H.; Zhou, H.; Ye, Z. Y.; Luo, S.; Sun, Z.; Sun, F. H.; Wang, J. W.; Xu, H. L.; Xu, H. X.; Chen, Z. H.; et al. Ultrafast Dynamics of Exciton-Polariton in Optically Tailored Potential Landscapes at Room Temperature. *J. Phys.: Condens. Matter* **2022**, *34* (2), No. 024001.
(54) Lai, C. W.; Kim, N. Y.; Utsunomiya, S.; Roumpos, G.; Deng, H.; Fraser, M. D.; Byrnes, T.; Recher, P.; Kumada, N.; Fujisawa, T.; Yamamoto, Y. Coherent zero-state and p-state in an exciton-polariton condensate array. *Nature* **2007**, *450* (7169), 529−532.
(55) Zhang, X. H.; Zhang, Y. J.; Dong, H. X.; Tang, B.; Li, D. H.; Tian, C.; Xu, C. Y.; Zhou, W. H. Room temperature exciton-polariton condensate in an optically-controlled trap. *Nanoscale* **2019**, *11* (10), 4496−4502.

https://doi.org/10.1021/acs.nanolett.1c04800
Nano Lett. 2022, 22, 2023−2029